



# UTL titanosilicate: An extra-large pore epoxidation catalyst with tunable textural properties

Jan Přech\*, Jiří Čejka

J. Heyrovský Institute of Physical Chemistry, Academy of Sciences of the Czech Republic, v.v.i., Dolejškova 3, CZ-182 23 Prague 8, Czech Republic

## ARTICLE INFO

### Article history:

Received 15 July 2015

Received in revised form 8 September 2015

Accepted 10 September 2015

Available online xxxx

### Keywords:

Titanosilicate UTL

Top-down synthesis

Epoxidation

Catalysis

Cyclooctene

## ABSTRACT

The UTL titanosilicate was prepared together with related lamellar Ti-IPC-1PISi material and zeolites Ti-IPC-2 (OKO) and Ti-IPC-4 (PCR) via top-down synthesis. The titanium can be incorporated to the UTL framework by conventional hydrothermal synthesis and it does not affect the so-called ADOR chemistry of the UTL material. Silica-titania pillaring concept was successfully applied providing very active Ti-IPC-1PITi catalyst for bulky molecules epoxidation with hydrogen peroxide. The textural properties of catalysts prepared can be tuned widely keeping the same crystalline titanosilicate active phase. All the materials were characterised by XRD, nitrogen sorption measurement, SEM, and DR-UV/vis spectroscopy. Ti-IPC-1PITi was the most active catalyst in cyclooctene, norbornene, and linalool epoxidation due to the lowest diffusion constraints and sufficient titanium content. Ti-UTL showed activity similar to Ti-BEA in epoxidation of cyclooctene and it provided different products than other titanosilicates in oxidation of linalool with hydrogen peroxide.

© 2015 Elsevier B.V. All rights reserved.

## 1. Introduction

Titanosilicate zeolites (e.g. TS-1 (MFI topology), Ti-BEA, Ti-MWW) represent valuable catalysts for epoxidation of C=C double bonds in organic molecules with both organic hydroperoxides and hydrogen peroxide as oxidation agents. The discovery of the TS-1 by Taramasso et al. [1] was a considerable breakthrough in the field of oxidation catalysis. Since that, a number of titanosilicates with 10-ring and 12-ring channels has been developed [2]; however, these suffer from diffusion limitations for bulky substrates. Therefore, titanosilicates with enhanced accessibility of the active sites, namely extra-large pore titanosilicates (possessing 14-ring channels) and lamellar titanosilicates, are subject of interest.

Lamellar titanosilicates possess the active Ti sites on the external surface of the crystalline layers and these are accessible without diffusion restrictions of the channel system [3]. Corma et al. incorporated titanium into lamellar ITQ-6 (FER structure) and demonstrated its activity in epoxidation of 1-hexene and norbornene [4]. Fan et al. prepared Ti-YNU-1 (possessing a structure similar to MWW-lammelar precursor) and this material exhibited enhanced activity in epoxidation of C<sub>5</sub>–C<sub>8</sub> cycloalkenes in comparison with 3-dimensional Ti-MWW (Si/Ti = 45) and Ti-BEA (Si/Ti = 35), although it had a Si/Ti ratio as high as 240 (e.g. cycloheptene TON:

Ti-YNU-1 1100 vs. Ti-MWW 50). These results demonstrated the potential of lamellar titanosilicates for oxidation of bulky molecules [5]. Kim et al. described a preparation of Ti-MCM-36 (MWW layers) catalyst by swelling of the Ti-MCM-22P layers with a surfactant and supporting of the layers (pillaring) with amorphous silica. The pillaring preserves the layer separation after removing of the surfactant by calcination. This pillared material exhibited more than 3 times higher TON than conventional TS-1 (Ti-MCM-36: 257, TS-1: 81) in 1-hexene epoxidation at 45 °C [6]. Ryoo et al. synthesised nanosheet TS-1 using a specially designed surfactant template (C<sub>18</sub>H<sub>37</sub>-N<sup>+</sup>(CH<sub>3</sub>)<sub>2</sub>-C<sub>6</sub>H<sub>12</sub>-N<sup>+</sup>(CH<sub>3</sub>)<sub>2</sub>-C<sub>6</sub>H<sub>13</sub> OH<sub>2</sub><sup>-</sup>) instead of conventional tetrapropylammonium hydroxide [7]. Nanosheet TS-1 exhibits an order of magnitude higher activity in epoxidation of cyclohexene and cyclooctene in comparison with conventional TS-1 (cyclooctene conversion: nanosheet TS-1 15.3% vs. TS-1 0.6% at 60 °C after 2 h) [7]. Xiao et al. prepared Ti-COE-4 material by inter-layer silylation of lamellar Ti-RUB-36 with dimethyldichlorosilane. Ti-COE-4 possesses free hydroxyl groups on the silane bridges between the layers and it is an active catalyst of 1-hexene (conversion 14.2% at 60 °C after 4 h vs. TS-1: conversion 21.2%) and cyclohexene oxidation (conversion 14% at 60 °C after 4 h vs. TS-1: conversion 2.3%). The main products of the oxidation over Ti-COE-4 were 1-hexene-3-one and 2-cyclohexen-1-ol respectively [8]. Recently, our group reported pillaring of the TS-1 nanosheets with tetratethyl orthosilicate (TEOS) or its mixture with titanium (IV) butoxide (Ti(OBu)<sub>4</sub>). The addition of Ti(OBu)<sub>4</sub> (0.05 eq based on TEOS) into the pillaring mixture led to a strong increase in the yield

\* Corresponding author. Tel.: +420 266 053 856.

E-mail address: [jan.prech@jh-inst.cas.cz](mailto:jan.prech@jh-inst.cas.cz) (J. Přech).

of cyclooctene oxide over silica-titania pillared lamellar TS-1 (TS-1-PITi, titanosilicate-1 silica-Titania Pillared) catalyst being 16.9% after 4 h in contrast to silica pillared lamellar TS-1 (TS-1-PI, yield 3.5%) [9].

From extra-large pore zeolites, only Ti-DON [10] and Ti-CFI [11] extra-large pore titanosilicates, both having 1-dimensional channels, has been reported until now. Ti-DON proved to be active catalyst in cyclohexane oxidation with both hydrogen peroxide and tert-butyl hydroperoxide [12] at room temperature. The Ti-CFI provided conversion of cyclooctene 21% and cyclooctene oxide yield 5.3% after 3 h at 60 °C.

We turned our attention towards an extra-large pore germanosilicate UTL containing 14-ring channels intersecting 12-ring channels. This material can be prepared with a number of trivalent heteroelements (B, Al, Ga, Fe, In) incorporated into the crystal framework [13]. This is a promising feature, because isomorphous incorporation of titanium into a zeolitic framework is a complex problem with many variables affecting the final outcome. Furthermore, the UTL zeolite can be converted into a number of related materials [14]. The structure can be disassembled into lamellar precursor IPC-1P (Institute of Physical Chemistry -1 precursor) by hydrolysis of germanium rich D4R units connecting germanium poor dense crystalline layers. The IPC-1P material may be turned into sub-zeolite IPC-1 or swollen and pillared, forming material IPC-1PISi (Institute of Physical Chemistry -1 Silica Pillared) [15]. Furthermore, it can be reassembled into OKO and PCR zeolites with smaller channels (12 × 10 resp. 10 × 8-ring 2-dimensional channel systems) [16] and a proper intercalation of the IPC-1P provides a 'shift' of the layers forming two new zeolites IPC-9 and IPC-10 with unique channel systems (two-dimensional with 10 × 7 resp. 12 × 9 rings) [17]. This, so-called, ADOR chemistry of the UTL zeolite has been reviewed in detail recently in Ref. [18].

In this contribution, we report on the preparation of UTL titanosilicate (Ti-UTL) and its transformations to lamellar Ti-IPC-1PISi material and titanosilicates Ti-IPC-2 (OKO structure) and Ti-IPC-4 (PCR structure). Silica-titania pillaring of the Ti-IPC-1P, in the same way as the preparation of TS-1-PITi (vide supra), is also presented. The activity of the catalysts is demonstrated in epoxidation of a group of linear and cyclic olefins (linalool, cyclooctene and norbornene) with hydrogen peroxide as the oxidant.

## 2. Experimental

### 2.1. Synthesis of Ti-UTL

The Ti-UTL was prepared using a procedure reported earlier [13]. The titanium was introduced into the framework directly during the hydrothermal synthesis. The initial gel with Si/Ti molar ratio (Si/Ti) 50 was prepared from Cab-O-Sil M5 silicon oxide (Havel Composites, Czech Republic), titanium (IV) butoxide ( $Ti(OBu)_4$ , Aldrich, 97%), germanium oxide (Alfa Aesar, Germany, 99.999%), distilled water, and (6R,10S)-6,10-dimethyl-5-azoniaspiro[4.5]decane hydroxide as a structure directing agent (SDA). The preparation of the SDA is described in Ref. [19]. The aqueous solution of the SDA was diluted with water and Cab-O-Sil M-5 and  $GeO_2$  were added under stirring. After 30 minutes of homogenisation,  $Ti(OBu)_4$ , diluted 1:3 with 1-butanol, was added dropwise and the gel was stirred for another 30 minutes. The initial molar composition of the synthesis gel was 2  $Ti(OBu)_4$ :50  $GeO_2$ :50 SDA:100  $SiO_2$ :3750  $H_2O$ . The zeolite crystallised in a 90-ml Teflon-lined autoclave at 175 °C under agitation for 7 days. The final product was filtered off, washed with water, dried at 85 °C and finally calcined with a stepwise increase of the temperature. At first at 200 °C for 2 h, then at 350 °C for 4 h and finally at 550 °C for 8 h, using a temperature ramp of 2 °C/min.

The synthesis of B-UTL, which was used as a parent material in the preparation of IPC-1TiPi catalyst, is described in Ref. [15].

### 2.2. Post-synthesis modifications

All the post-synthesis modifications of the Ti-UTL were performed according to procedures reported earlier [15,16]. The Ti-UTL was converted into lamellar Ti-IPC-1P by hydrolysis of the germanium D4R units with 0.01 M HCl. 250 ml of the HCl solution were used per 1 g of the calcined Ti-UTL and the material was hydrolysed at 75 °C for 16 h under agitation. The resulting lamellar precursor Ti-IPC-1P was collected by filtration, washed with water and dried at 65 °C.

The Ti-IPC-1PISi and Ti-IPC-1PITi (Institute of Physical Chemistry -1 silica-Titania Pillared) samples were prepared in a following way. The Ti-IPC-1P was swollen with a solution of cetyltrimethylammonium hydroxide (CTMA OH, 30 g/g of the Ti-IPC-1P). The swelling occurred at room temperature for 24 h under stirring. The swollen product was centrifuged, washed with water and dried at 65 °C. The pillaring was done using tetraethyl orthosilicate (TEOS) or its mixture with  $Ti(OBu)_4$  to form pillared lamellar Ti-IPC-1PISi resp. Ti-IPC-1-PITi catalyst. 10 ml of the pillaring medium were used per 1 g of the swollen material and the mixture was stirred at 85 °C for 24 h. Then the mixture was centrifuged and the solid material was dried for 48 h at room temperature. Subsequently, the product was hydrolysed in water with 5% of ethanol (100 ml/1 g) at ambient temperature for 24 h under vigorous stirring. Finally, the solid material was centrifuged again, dried at 65 °C and calcined in an air flow at 550 °C for 8 h using a temperature ramp of 2 °C/min.

The Ti-IPC-2 catalyst was prepared by stabilisation of the Ti-IPC-1P with diethoxydimethylsilane in 1 M  $HNO_3$  in a 25-ml Teflon-lined autoclave at 175 °C for 16 h without agitation. 10 ml of the  $HNO_3$  solution and 0.5 g of the diethoxydimethylsilane were used per 1 g of the Ti-IPC-1P. The strongly hydrophobic product was obtained. Final calcination was performed at 550 °C for 8 h using a temperature ramp of 2 °C/min.

The Ti-IPC-4 was formed via intercalation of the Ti-IPC-1P with 1-aminoctane. 1 g of the Ti-IPC-1P was mixed with 30 ml of 1-aminoctane (Aldrich, 99%) and stirred at 90 °C for 16 h. The solid material was centrifuged and dried at room temperature for 24 h. Finally the material was calcined at 750 °C for 8 h with a temperature ramp of 2 °C/min.

### 2.3. Synthesis of TS-1 and Ti-BEA

Conventional titanosilicate TS-1 (3D TS-1) was prepared from a gel with initial Si/Ti ratio 40 according to the procedure described in Ref. [20] using tetraethyl orthotitanate (Aldrich, technical grade) and tetraethyl orthosilicate with tetrapropylammonium hydroxide (Aldrich, 20% in water) as a structure directing agent.

Ti-BEA was prepared from a gel with initial Si/Ti ratio 80, according to the procedure described in Ref. [21], using tetraethyl orthosilicate and tetraethyl orthotitanate (Aldrich, technical grade) in the presence of hydrogen peroxide (Aldrich, 35% in water) with tetraethylammonium hydroxide (Aldrich, 40% in water) as a structure directing agent.

### 2.4. Characterisation techniques

X-ray powder diffraction (XRD) patterns were collected using a Bruker AXS D8 Advance diffractometer equipped with a graphite monochromator and a position sensitive detector Väntec-1 using  $CuK\alpha$  radiation in Bragg–Brentano geometry. Data were collected in continuous mode over the  $2\theta$  range of 1–40° with a step size of 0.00853° and time per step 0.25 s.

The size and shape of zeolite crystals were examined by scanning electron microscopy (SEM) on a JEOL, JSM-5500LV microscope. The images were collected with acceleration voltage of 20 kV.

Nitrogen sorption isotherms were measured at liquid nitrogen temperature ( $-196^{\circ}\text{C}$ ) with Micromeritics Gemini volumetric instrument. Prior to the sorption measurements, individual zeolites were outgassed in a stream of helium at  $300^{\circ}\text{C}$  for 3 h.

BET area was evaluated using adsorption data in the range of a relative pressure from  $p/p_0 = 0.05$  to  $p/p_0 = 0.20$ . The  $t$ -plot method [22] was applied to determine the volume of micropores ( $V_{\text{micro}}$ ). The adsorbed amount of nitrogen at  $p/p_0 = 0.95$  reflects the total adsorption capacity ( $V_{\text{total}}$ ) of the material.

DR-UV/vis absorption spectra were collected using Perkin-Elmer Lambda 950 Spectrometer with 2 mm quartz tube and large 8 mm  $\times$  16 mm slit. The data were collected in the wavelength range of 190–500 nm. All the samples were analysed after calcination.

Chemical composition of the materials (expressed hereafter as a Si/Ti ratio) was determined by ICP-OES ThermoScientific iCAP 7000 instrument.

## 2.5. Catalytic tests

The epoxidations of cis-cyclooctene (Aldrich, 95%), norbornene (Aldrich, 99%), and linalool (Aldrich, 97%) were carried out in a 25 ml magnetically stirred glass three-necked round bottom flask equipped with a Dimroth condenser at  $60^{\circ}\text{C}$ . The alkene/catalyst mass ratio was 10 ( $S/C = 10$ ) and alkene/ $\text{H}_2\text{O}_2$  molar ratio was 2. Acetonitrile (Fisher chemical, HPLC grade) and methanol (Fisher chemical, HPLC grade) were used as solvents and mesitylene (99%, Acros-Organics) served as an internal standard. In a standard experiment, 500 mg of norbornene or cyclooctene were mixed with 250 mg of the internal standard, 50 mg of the catalyst and 6.65 ml of acetonitrile. The reaction was started by addition of  $\text{H}_2\text{O}_2$  aqueous solution (35 wt.%, Aldrich) into the mixture. Epoxidation of linalool (6 mmol, 0.925 g) was performed in methanol (9 ml) using 60 mg of the catalyst ( $S/C = 15$ ) and 250 mg of the internal standard. The reaction was started by addition of  $\text{H}_2\text{O}_2$  aqueous solution (1 molar eq of linalool) keeping the C=C double bond/ $\text{H}_2\text{O}_2$  ratio 2. Samples were taken in regular intervals, centrifuged, cooled and analysed using an Agilent 6850 GC system with 50 m long DB-5 column, an autosampler and a FID or a MS detector. Helium was used as a carrier gas. The results were compared with standard Ti-BEA and TS-1 catalysts.

## 3. Results and discussion

### 3.1. Catalyst structure

Well crystalline Ti-UTL zeolite has been prepared with the Si/Ti ratio 139. The XRD pattern of the material is presented in Fig. 1 and it is well consistent with standard UTL pattern [23]. The hydrolysis of the Ti-UTL led to a lamellar precursor denoted Ti-IPC-1P. Most of the diffraction lines disappeared with the structure disassembly. A shift of the most intensive (2 0 0) reflection towards higher angles can be observed between the Ti-UTL and Ti-IPC-1P. It characterises the d-spacing of 2.9 nm and 2.1 nm, respectively. When the Ti-IPC-1P was swollen with a solution of cetyltrimethylammonium hydroxide, intensive reflections (1 0 0), (2 0 0) and (3 0 0) appeared in the diffraction pattern, indicating the extension of the d-spacing to 3.7 nm. The interlayer distance of the swollen material is preserved also in the pillared Ti-IPC-1PISi material (Fig. 1). The Si/Ti ratio increased to 480 in Ti-IPC-1P. This is a result of the removal of part of the crystalline material during D4R hydrolysis together with dilution of the titanosilicate phase by the amorphous silica used for

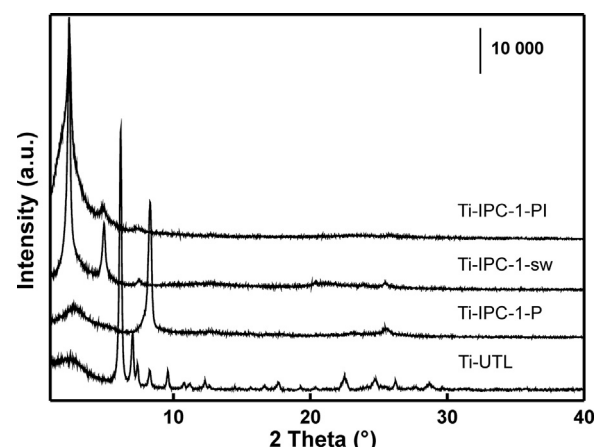


**Fig. 1.** Powder XRD patterns of parent Ti-UTL, lamellar precursor Ti-IPC-1P, lamellar precursor after swelling Ti-IPC-1-sw and pillared calcined Ti-IPC-1PISi material.

the pillaring. A scheme describing the post-synthesis treatment is presented in the Supporting information (Fig. S1).

The Ti-IPC-1P lamellar precursor can be directly calcined forming a sub-zeolite Ti-IPC-1. The crystalline layers of Ti-IPC-1 are oriented randomly one on another with a d-spacing of 1.9 nm (calculated from (2 0 0) reflection, Fig. 2). Stabilisation of the Ti-IPC-1P with diethoxydimethylsilane in 1 M  $\text{HNO}_3$  at  $175^{\circ}\text{C}$  and subsequent calcination resulted in the formation of Ti-IPC-2 material [16] with the OKO topology and Si/Ti ratio 210. The XRD pattern is presented in Fig. 2. The increase in the Si/Ti ratio with respect to the parent Ti-UTL results from the introduction of purely siliceous S4R units during the stabilisation.

Intercalation of the Ti-IPC-1P with 1-aminoctane enables to organise the layers leading to the formation of titanosilicate Ti-IPC-4 (PCR topology). The XRD pattern is presented in Fig. 2. The Ti-IPC-4 material possesses narrow 10-ring intersecting 8-ring pores. In general, the introduction of Ti into the UTL structure did not affect the possibility of its top-down transformations as described in Ref. [15,16].

Having in mind the low titanium content in the Ti-IPC-1PISi material as the most promising catalyst in the term if active sites accessibility, we used the same approach as in the case of silicatitania pillared lamellar TS-1 [9]. Therefore, a set of materials denoted Ti-IPC-1PITi has been prepared, where different amounts of  $\text{Ti(OBu)}_4$  were added into the TEOS used for the pillaring treatment (typically in the range Si/Ti 30–100). One sample of IPC-1P without titanium present form the hydrothermal synthesis was

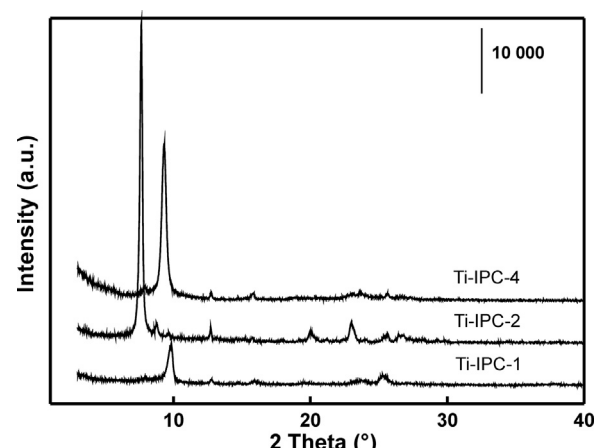


**Fig. 2.** Powder XRD patterns of calcined Ti-IPC-1, Ti-IPC-2 and Ti-IPC-4 materials.

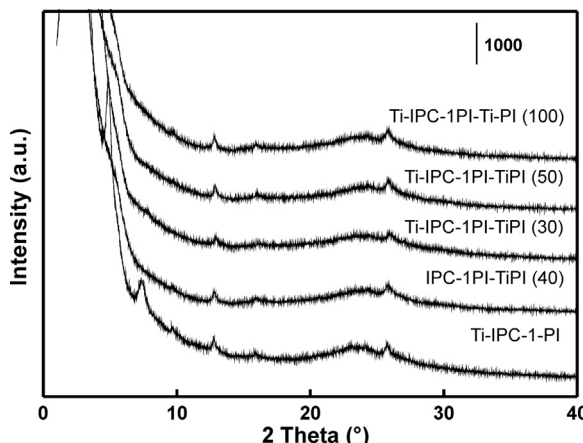


**Fig. 3.** Powder XRD patterns of Ti-IPC-1-PITi samples with different composition of the pillaring medium.

prepared in this way (denoted IPC-1PITi) from B-UTL with initial Si/B ratio 27 as well. A comparison of their XRD patterns with silica-pillared Ti-IPC-1PISi is shown in Fig. 3. Two weak diffraction lines at  $2\theta = 12.8^\circ$  and  $25.7^\circ$  are the main features of the pattern and their intensities are similar for all the samples.

Scanning electron micrographs (SEM), showed in Fig. 4, reveal characteristic thin plate shape of the Ti-UTL crystals (a). This morphology is preserved also during the post-synthesis modifications. In the case of the pillared samples (b, c), the crystals are partially covered with amorphous silica resp. silica-titania phase resulting from the excess of the pillaring medium. The thin plate morphology is characteristic also for the Ti-IPC-2 (d).

The textural properties and Ti content of all discussed samples are listed in Table 1. Selected nitrogen sorption isotherms are presented in Fig. 5. The positions of the isotherms belonging to

**Table 1**  
Textural properties and Ti content of the Ti-UTL and derived catalysts.

Titanosilicate	BET ( $\text{m}^2/\text{g}$ )	$V_{\text{mic}}$ ( $\text{ml/g}$ )	$V_{\text{tot}}$ ( $\text{ml/g}$ )	Si/Ti
Ti-UTL	539	0.239	0.29	139
Ti-IPC-1-PI	1001	0	0.67	480
Ti-IPC-1	192	0.07	0.13	n.d. <sup>a</sup>
Ti-IPC-2	383	0.15	0.22	210
Ti-IPC-4	237	0.10	0.15	n.d. <sup>a</sup>
IPC-1-PITi (40) <sup>b</sup>	664	0.11	0.34	43
Ti-IPC1-PITi (30) <sup>b</sup>	910	0	0.46	16
Ti-IPC1-PITi (50) <sup>b</sup>	662	0.14	0.35	18
Ti-IPC1-PITi (100) <sup>b</sup>	763	0.10	0.43	69
Ti-BEA	339	0.14	0.19	116
TS-1	450	0.13	0.16	44

<sup>a</sup> Ti content was not determined because the material was not intended to be used in catalytic tests.

<sup>b</sup> Si/Ti molar ratio of the pillaring medium is given in brackets.

different titanosilicate samples demonstrate the possibilities of the texture tuning. All the presented materials were prepared from one parent Ti-UTL zeolite. The Ti-UTL, Ti-IPC-2, and Ti-IPC-4 materials exhibit type I isotherms, typical for microporous materials. The isotherm of Ti-IPC-1 is also type I, although its pores are disordered [18]. The BET areas, micropore volumes, ( $V_{\text{mic}}$ ) and total adsorption capacities ( $V_{\text{tot}}$ ) decrease with decreasing size of the pores in the order Ti-UTL > Ti-IPC-2 > Ti-IPC-4 > Ti-IPC-1 (e.g. BET area: Ti-UTL =  $539 \text{ m}^2/\text{g}$ , Ti-IPC-2 =  $383 \text{ m}^2/\text{g}$ , Ti-IPC-4 =  $237 \text{ m}^2/\text{g}$ , Ti-IPC-1 =  $192 \text{ m}^2/\text{g}$ ). The swelling and pillaring treatment of Ti-IPC-1P lead to a material with BET area up to  $1001 \text{ m}^2/\text{g}$  (Ti-IPC-1PI). This material possesses no micropores because it consists only of dense layers supported by amorphous silica pillars. The addition of titanium during the pillaring resulted in a decrease in the BET area and adsorption capacity and in some cases in formation of some micropores. The Si/Ti molar ratio of the pillaring medium for different samples is given in brackets. We ascribe this observation to higher reactivity of  $\text{Ti(OBu)}_4$  in comparison with the TEOS [24]

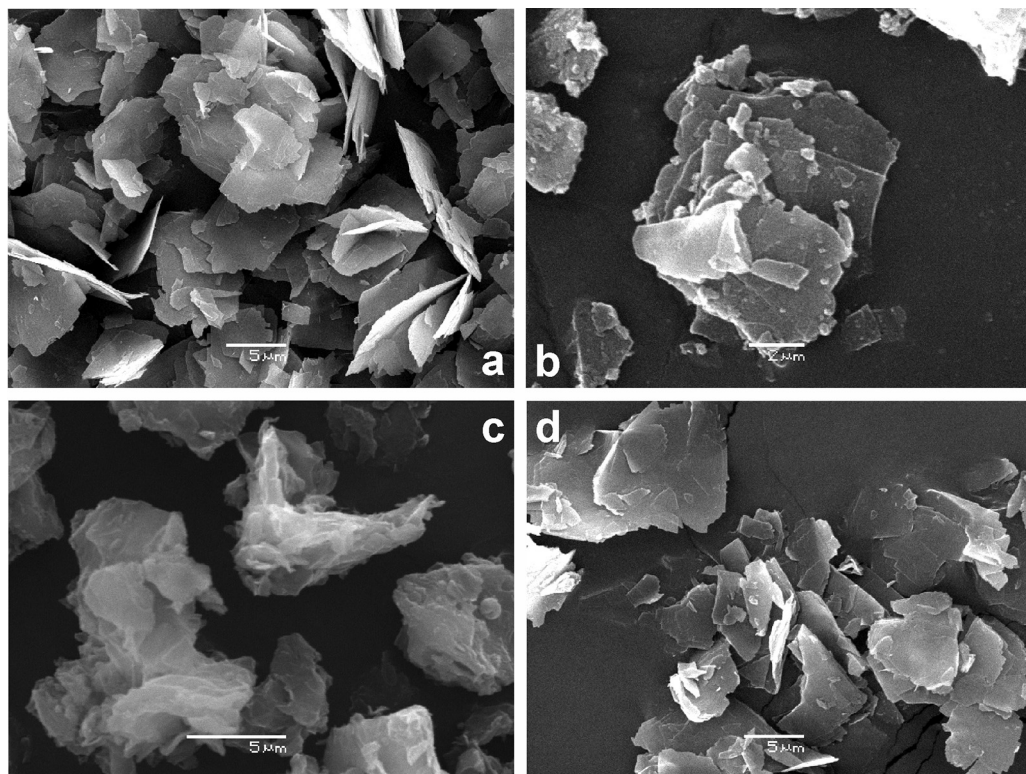


**Fig. 4.** SEM micrographs of catalysts Ti-UTL (a), Ti-IPC-1PISi (b), Ti-IPC-1PITi (c) and Ti-IPC-2 (d).

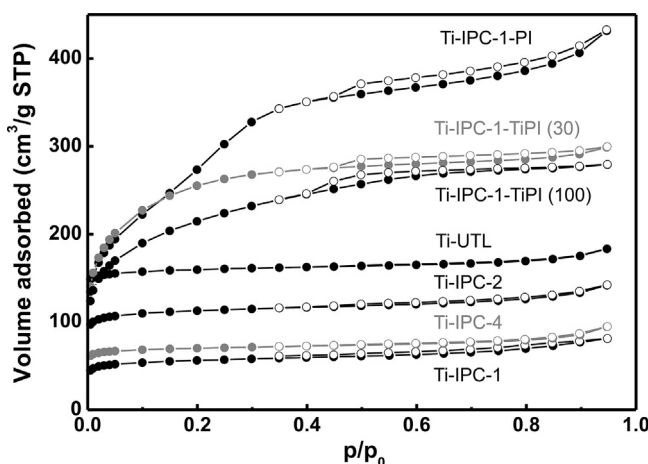


**Fig. 5.** Nitrogen sorption isotherms of the Ti-UTL and derived materials. Empty points denote desorption. Number in brackets indicate Si/Ti ratio of the pillaring medium.

and it is consistent with our experience with lamellar TS-1 pillaring [9]. The titanium containing pillars are thicker. The shape of the isotherms, which belong to the pillared samples, is typical for these materials. The increase in the amount of adsorbed nitrogen in the range of  $p/p_0$  0.05–0.4 is typical for the filling of the interlayer space, which belongs to the region of small mesopores [25]. Once this space is filled, the nitrogen uptake is strongly diminished.

The coordination of titanium in the discussed catalysts was investigated by DR-UV/vis spectroscopy. It is generally assumed that isolated framework tetrahedrally coordinated titanium species are the active sites in the epoxidation reactions [26]. The DR-UV/vis spectra of the Ti-UTL derived catalysts are presented in Fig. 6. All the spectra were collected in air after calcination.

The most intensive absorption band in the spectra of Ti-UTL (a), Ti-IPC-2 (b), Ti-IPC-1PISi (c), Ti-BEA (i) and TS-1 (j) is centred between 205 and 210 nm. Zecchina et al. ascribed this band to tetrahedrally coordinated framework  $\text{Ti}(\text{OSi})_4$  species [27]. That means the titanium is incorporated into the framework during the hydrothermal synthesis. It is known that there exists a limit for the titanium amount which can be incorporated into the framework of TS-1 [28]. Similarly, we expect there exists a limit in the case of Ti-UTL. A weak absorption above 300 nm in the spectrum of Ti-UTL (Fig. 6a) may indicate that the Ti content in the sample is close to the UTL limit of titanium incorporation. The spectra of silicate-titania pillared samples (Fig. 6d, e, f, h) exhibit another intensive absorption band between 240 and 290 nm. This absorption results from presence of penta- or hexa-coordinated extra-framework  $\text{Ti}(\text{OH})(\text{OSi})_3(\text{H}_2\text{O})$  and  $\text{Ti}(\text{OH})_2(\text{OSi})_2(\text{H}_2\text{O})_2$  species [29]. The catalytic activity of these species is a subject of debate and it is believed that extra-framework species with coordination number 5 and 6 are inactive [2]. However, there exists some indicia that non-tetrahedral titanium species might be active in oxidation catalysis as-well [30–32]. A shoulder above 300 nm can be observed additionally to the bands mentioned in the above discussion. It points to a presence of a certain amount of anatase-like  $\text{TiO}_2$  phase containing  $\text{Ti}-\text{O}-\text{Ti}$  species (absorbing at typically at 330 nm). The anatase-like species are known to be inactive or to cause unproductive  $\text{H}_2\text{O}_2$  decomposition during the epoxidation reaction [2]. The observed catalytic performance is discussed below.

An attempt to prepare Ti-IPC-2 material by stabilisation with  $\text{Ti}(\text{OBu})_4$  instead of diethoxydimethylsilane was performed, but only a disordered Ti-IPC-1 was obtained (denoted Ti-IPC-1-Ti-stab), containing high amount of anatase phase. Its DR-UV/vis spectrum is shown in Fig. 6g.

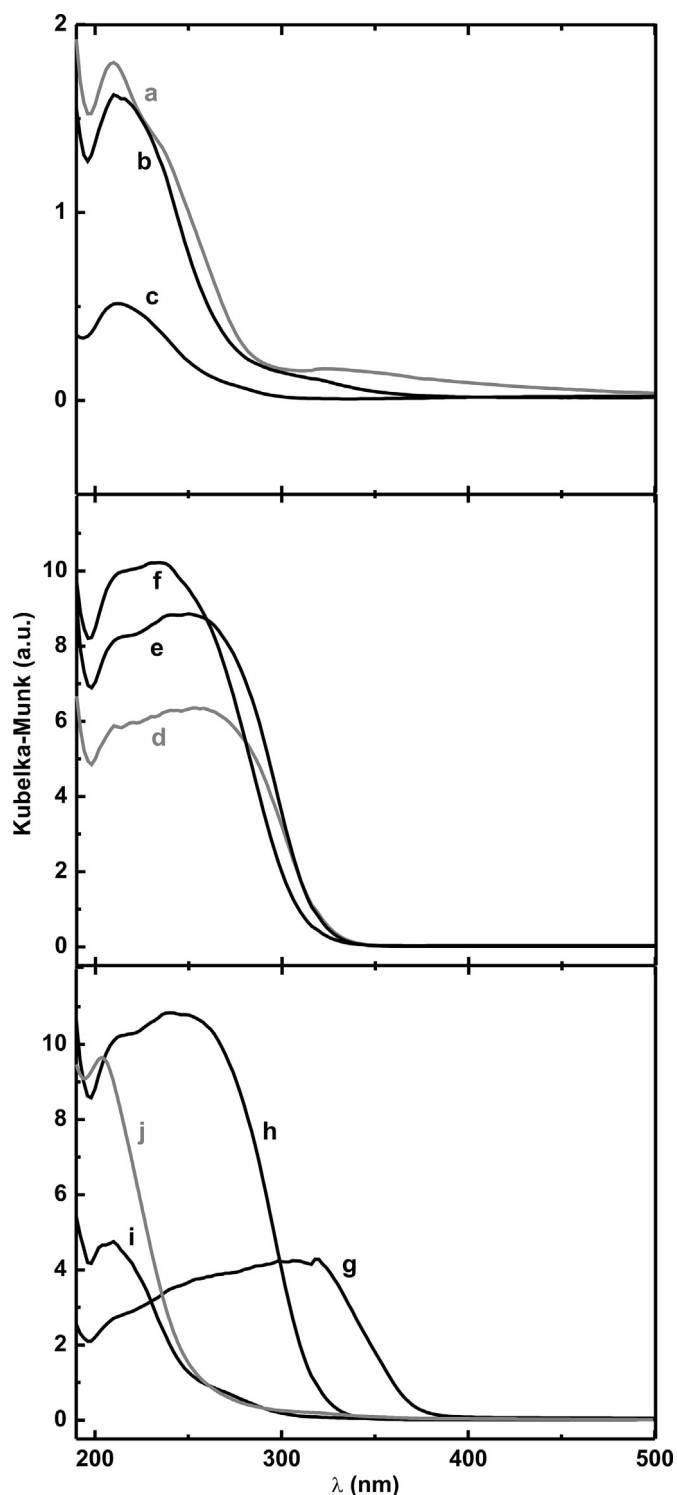


**Fig. 6.** DR-UV/vis spectra of the discussed titanosilicates. (a) Ti-UTL, (b) Ti-IPC-2, (c) Ti-IPC-1PISi, (d) Ti-IPC-1PITi (30), (e) Ti-IPC-1PITi (50), (f) Ti-IPC-1PITi (100), (g) Ti-IPC-1-Ti-stab, (h) IPC-1PITi (40), (i) Ti-BEA, (j) TS-1.

### 3.2. Catalytic tests

The Ti-UTL derived catalysts were tested in epoxidation of cyclooctene, norbornene, and linalool at 60 °C with hydrogen peroxide as the oxidant. The results are compared with Ti-BEA and TS-1 catalysts as benchmarks (Table 2). The Ti-UTL provided a yield of cyclooctene oxide 4.7% after 4 h what is similar to the large-pore Ti-BEA catalyst with similar Ti content (Si/Ti 139 resp. 116). The

**Table 2**

Epoxidation of cyclooctene, norbornene and linalool at 60 °C for 4 h.

Entry	Catalyst	Substrate	Solvent	X <sub>(Substrate)</sub> (%) <sup>a</sup>	y <sub>(Epoxide)</sub> (%) <sup>b</sup>	S(X) (%) <sup>c</sup>
1	Ti-UTL	Cyclooctene	Acetonitrile	14.3	4.7	30 (20%)
2	Ti-IPC-1PI	Cyclooctene	Acetonitrile	21.3	8.0	38 (20%)
3	Ti-IPC-2	Cyclooctene	Acetonitrile	11.2	0.4	n.d. <sup>e</sup>
4a	Ti-IPC-1PITi (30)	Cyclooctene	Acetonitrile	26.0 <sup>d</sup>	19.5 <sup>d</sup>	–
4b	Ti-IPC-1PITi (30)	Cyclooctene	Acetonitrile	35.8	23.3	80 (20%)
5	Ti-IPC-1PITi (50)	Cyclooctene	Acetonitrile	29.0	16.1	65 (20%)
6	Ti-IPC-1PITi (100)	Cyclooctene	Acetonitrile	34.7	24.7	80 (20%)
7	IPC-1PITi (40)	Cyclooctene	Acetonitrile	28.3	15.5	67 (20%)
8	Ti-IPC-1PITi (30)	Cyclooctene	Methanol	34.8	19.1	78 (20%)
9	Ti-BEA	Cyclooctene	Acetonitrile	14.0	4.7	32 (20%)
10	TS-1	Cyclooctene	Acetonitrile	5.9	2.9	55 (10%)
11	Ti-IPC-1PITi (30)	Norbornene	Acetonitrile	57.2	12.6	30 (20%)
12	Ti-UTL	Norbornene	Acetonitrile	60.5	0.9	n.d. <sup>e</sup>
13	Ti-IPC1-1PI	Norbornene	Acetonitrile	49.2	6.5	19 (20%)
14	Ti-BEA	Norbornene	Acetonitrile	54.3	3.8	8.0 (10%)
15	Ti-UTL	Linalool	Methanol	31.7	3.3 <sup>f</sup>	9 (10%)
16	Ti-IPC1-1PI	Linalool	Methanol	6.4	3.8 <sup>f</sup>	64 (10%)
17	Ti-IPC-1PITi (30)	Linalool	Methanol	46.6	23.5 <sup>f</sup>	50 (10%)
18	Ti-IPC1-1PITi (100)	Linalool	Methanol	43.5	22.2 <sup>f</sup>	58 (10%)
19	TS-1	Linalool	Methanol	3.0	3.0 <sup>f</sup>	n.d. <sup>e</sup>

<sup>a</sup> Conversion of the substrate after 4 h.<sup>b</sup> Yield of the epoxide after 4 h.<sup>c</sup> Selectivity of the reaction at the conversion in brackets; defined as [produced epoxide]/[consumed substrate].<sup>d</sup> Conversion and yield given after 1 h of the reaction.<sup>e</sup> Selectivity was not determined due to low conversion or yield.<sup>f</sup> Yield is calculated for 2-(5-methyl-5-vinyltetrahydro-1-furyl)-2-propanol, the main product of in-situ rearrangement of the 6,7-epoxylinalool.

selectivity of the reaction was 30–32% at 20% conversion (reached after 8.3 h) for both catalysts. The transformation of the Ti-UTL into a pillared material Ti-IPC-1PISi resulted in an increase in the yield (8% after 4 h with Ti-IPC-1PI) as well as the selectivity (38% at 20% conversion), although the active phase was diluted by the pillaring treatment. We ascribe this to lower diffusion restrictions of the Ti-IPC-1PISi material. The yield of cyclooctene oxide over Ti-IPC-2 was only 0.4% after 4 h (less than the yield over TS-1: 2.9%). We expect that this is a result of both diffusion restrictions in 12 × 10-ring channel system and low titanium content. When silica-titania pillared catalysts were tested, both yield of the cyclooctene oxide and the selectivity of the reaction increased dramatically. The highest yields of the epoxide after 4 h were obtained using Ti-IPC-1PITi (30) and Ti-IPC-1PITi (100) catalysts (23.3% resp. 24.7) with 80% selectivity at 20% conversion. It should be noted that these catalysts are those possessing the highest BET area (910 resp. 763 m<sup>2</sup>/g) and total adsorption capacities (0.46 resp. 0.43 ml/g) among the silica-titania pillared catalysts (Table 1). In other words, the catalysts with most open structures and therefore the lowest diffusion limitations exhibited the highest yields. The conversion and yield are independent on the titanium content among the silica-titania pillared catalysts, but there exists a linear dependence of the cyclooctene conversion on the total adsorption capacity. Lower conversion (29% after 4 h) and yield (16.1% after 4 h) obtained using the Ti-IPC-1PITi (50) (BET = 662 m<sup>2</sup>/g, V<sub>tot</sub> = 0.35 m<sup>2</sup>/g) well confirms this hypothesis. We conclude that the open structure of the catalyst allows the reactants to access the active sites rapidly (resulting in high conversion in comparison with the others) and on the other hand allow the products to leave rapidly preventing their further conversion on the titanium sites [29] reaching therefore high selectivity. The IPC-1PITi (40) catalyst (possessing no titanium from the hydrothermal synthesis) fits to the group of Ti-pillared catalysts providing conversion and yield of 28.3% resp. 15.5% after 4 h. Its UV/vis spectrum is also similar to the other Ti-pillared catalysts (Fig. 6). This is very close to the results obtained over Ti-IPC-1PITi (50) (possessing also similar textural properties: BET = 662 m<sup>2</sup>/g vs. 664 m<sup>2</sup>/g, V<sub>tot</sub> = 0.35 m<sup>2</sup>/g vs. 0.34 m<sup>2</sup>/g). We expect boron atoms were washed out during the hydrolysis of the starting B-UTL and titanium atoms have been

incorporated into vacancies after boron atoms similarly to the Ref. [30].

Furthermore, we expect that some impregnation of the crystalline layers with titanium species occurred during the silica-titania pillaring and at least a part of those new Ti centres is catalytically active. On the other hand, the activity of the titanium in the pillars is questionable, because the sites which are not located on the surface might be inaccessible.

In the epoxidation over Ti-IPC-1PITi (30) as a representative catalyst, methanol was used as a solvent instead of acetonitrile; however, the change of the solvent did not influence the conversion significantly (see Table 2 entry 4b (acetonitrile) vs. entry 8 (methanol): cyclooctene conversion 35.8% vs. 34.7%). Only the yield of the epoxide decreased (23.3% vs. 19.1% after 4 h). This is in accordance with previous observations because the epoxide undergoes a ring-opening reaction with methanol [33]. Following the development of cyclooctene conversion and cyclooctene oxide yield in time over the Ti-IPC-1-PITi (30) as a representative catalyst, conversion of 26% and yield 19.5% were observed after 1 h (Table 2, entry 4a). Then the rate of the reaction decreased rapidly and after 4 h it stopped. The cyclooctene conversion at this time was 35.8% but a theoretical maximum conversion is 50% (0.5 eq of H<sub>2</sub>O<sub>2</sub> is used). Iodometric titration of the sample revealed total conversion of the hydrogen peroxide, which means, that approximately 28% of hydrogen peroxide was ineffectively decomposed (due to the presence of anatase-like phase) or consumed in some side reactions (e.g. further oxidation of the ring opening products observed by Pirovano et al. [34]). When a dose of fresh H<sub>2</sub>O<sub>2</sub> (0.5 eq base on initial substrate amount) was added after 3 h, the reaction was restored reaching cyclooctene conversion 53.7% and epoxide yield 30.7% after 5 h since the beginning of the experiment and cyclooctene conversion 86% and epoxide yield 40% after 24 h. Development of the conversion and yield in time during the reaction is presented in the supplementary information (Fig. S2).

The leaching test was performed with the Ti-IPC-1PITi (30) as a representative catalyst. The reaction mixture containing cyclooctene, mesitylene and hydrogen peroxide in acetonitrile reacted at 60 °C for 30 min reaching conversion of 12.9% and yield of

10%. Then the catalyst was separated from the reaction mixture by centrifugation (the temperature decreased to 45 °C during centrifugation) and the mixture was stirred further at 60 °C and samples were taken in 1 h intervals. No further formation of cyclooctene oxide was observed for 4 h confirming that the epoxidation do not occur in homogenous phase.

When norbornene was used as the substrate, the order of epoxide yields over different catalysts was similar to cyclooctene epoxidation: Ti-IPC-1PITi (30)  $y = 12.6\%$  > Ti-IPC-1PISi  $y = 6.5\%$  > Ti-BEA  $y = 3.8\%$  > Ti-UTL  $y = 0.9\%$  after 4 h. Norbornene is more rigid molecule in comparison with cyclooctene and therefore the advantage of 3-dimensional 12-ring channel system of the Ti-BEA over 2-dimensional system of Ti-UTL manifests itself.

Last but not least, the epoxidation of linalool was performed, using methanol as the solvent. Linalool possesses two different double bonds, which can be oxidised; however, only the oxidation of C6=C7 double bond was observed in all the reactions. The 6,7-epoxylinalool linalool is very reactive and it was never observed directly. It easily undergoes an acid catalysed intramolecular ring closing rearrangement with the free OH group [35]. The main product of the rearrangement is 2-(5-methyl-5-vinyltetrahydro-1-furyl)-2-propanol (known as linalool oxide) and minor product is 2,2-dimethyl-3-hydroxy-6-methyl-6-vinyltetrahydropyran. Yields and selectivity are calculated for the main product (2-(5-methyl-5-vinyltetrahydro-1-furyl)-2-propanol). Once more, the highest yield of the linalool oxide (23.5% after 4 h) was provided by the Ti-IPC-1PITi (30) catalyst. Only slightly lower yield was given by Ti-IPC-1PITi (100) but on the other hand, this catalyst was more selective (58% vs. 50% at 10% conversion). The Ti-IPC-1PISi catalyst was the most selective (64% at 10% conversion), but due to its low Ti content, the linalool oxide yield was only 3.8% after 4 h. The yield of linalool oxide over Ti-UTL was 3.3% after 4 h, but the conversion was unexpectedly high (31.7%). Two new products were observed instead of the products of 6,7-epoxylinalool rearrangement. Both substances were linalool derivates; however, it was not possible to determine their structure only from the GC-MS data and none of them is linalool epoxide or its simple ring opening product (diol or keton). We ascribe the change in the product composition to the presence of germanium in the Ti-UTL structure. All the discussed catalysts exceeded the performance of the TS-1 because it is difficult to enter the narrow TS-1 pores for the branched linalool.

#### 4. Conclusions

A new titanasilicate with the UTL layers was prepared. The presence of germanium-rich D4R units in its structure allows its transformation into Ti-IPC-1P lamellar precursor and subsequent reassembly into new titanasilicates Ti-IPC-2 and Ti-IPC-4 possessing the OKO and PCR topology respectively. These transformations were demonstrated and the resulting materials contained mainly titanium in the framework crystallographic positions. The Ti-IPC-1P was also swollen with cetyltrimethylammonium hydroxide and pillared with amorphous silica or silica-titania phase providing Ti-IPC-1PISi and Ti-IPC-1PITi materials with open structure and well accessible titanium sites located on the surface of the layers. All the materials were characterised by XRD, nitrogen sorption, SEM, and DR-UV/vis spectroscopy and successfully used as catalysts of cyclooctene, norbornene and linalool epoxidation. In general, the Ti-IPC-1PITi (30) was the most active catalyst and its performance in cyclooctene epoxidation exceeds conventional large pore Ti-BEA catalyst and also other active catalysts such as TS-1-PITi [9] and Ti-CON [30], prepared earlier by our group.

#### Acknowledgements

The authors acknowledge support of the Czech Science Foundation P106/12/G015. In addition, the authors thank to G. Sádovská for DR-UV/vis measurement and Valeryia Kasneryk for the SEM.

#### Appendix A. Supplementary data

Supplementary data associated with this article can be found, in the online version, at <http://dx.doi.org/10.1016/j.cattod.2015.09.036>.

#### References

- [1] M. Taramasso, G. Perego, B. Notari, US Pat 4410501 (1983).
- [2] T. Tatsumi, Metal-substituted zeolites as heterogenous oxidation catalysts, in: N. Mizuno (Ed.), *Modern Heterogenous Oxidation Catalysis*, Wiley-WCH, Weinheim, 2009, pp. 125–153.
- [3] W.J. Roth, P. Nachtigall, R.E. Morris, J. Čejka, *Chem. Rev.* 114 (2014) 4807–4837.
- [4] A. Corma, U. Diaz, M.E. Domíne, V. Fornes, *Chem. Commun.* (2000) 137.
- [5] W. Fan, P. Wu, S. Namba, T. Tatsumi, *Angew. Chem. Int. Ed.* 43 (2004) 238–242.
- [6] S. Kim, H. Ban, W. Ahn, *Catal. Lett.* 113 (2007) 160–164.
- [7] K. Na, Ch. Jo, J. Kim, W. Ahn, R. Ryoo, *ACS Catal.* 1 (2011) 901–907.
- [8] F.S. Xiao, B. Xie, H. Zhang, L. Wang, X. Meng, W. Zhang, X. Bao, B. Yilmaz, U. Müller, H. Gies, H. Imai, T. Tatsumi, D. De Vos, *ChemCatChem* 3 (2011) 1442–1446.
- [9] J. Přech, P. Eliášová, D. Aldhayan, M. Kubů, *Catal. Today* 243 (2015) 134–140.
- [10] K.J. Balkus Jr., A.G. Gabrielov, S.I. Zones, *Stud. Surf. Sci. Catal.* 97 (1995) 519–525.
- [11] J. Přech, M. Kubů, J. Čejka, *Catal. Today* 227 (2014) 80–86.
- [12] K.J. Balkus Jr., A.G. Gabrielov, Patent WO 9729046 A1 (1997).
- [13] M.V. Shamzhy, O.V. Shvets, M.V. Opanasenko, P.S. Yaremov, L.G. Sarkisyan, P. Chlubná, A. Zukal, V.R. Marthala, M. Hartmann, J. Čejka, *J. Mater. Chem.* 22 (2012) 15793–15803.
- [14] R.E. Morris, J. Čejka, *Nat. Chem.* 7 (2015) 381–388.
- [15] W.J. Roth, O.V. Shvets, M. Shamzhy, P. Chlubná, M. Kubů, P. Nachtigall, J. Čejka, *J. Am. Chem. Soc.* 133 (2011) 6130–6133.
- [16] W.J. Roth, P. Nachtigall, R.E. Morris, P.S. Wheatley, V.R. Seymour, S.E. Ashbrook, P. Chlubná, L. Grajciar, M. Položij, A. Zukal, O. Shvets, J. Čejka, *Nat. Chem.* 5 (2013) 628–633.
- [17] M. Mazur, P.S. Wheatley, M. Navarro, W.J. Roth, M. Položij, A. Mayoral, P. Eliášová, P. Nachtigall, J. Čejka, R.E. Morris, *Nat. Chem.* (2015), <http://dx.doi.org/10.1038/nchem.2374> (in press).
- [18] P. Eliášová, M. Opanasenko, P.S. Wheatley, M. Shamzhy, M. Mazur, P. Nachtigall, W.J. Roth, R.E. Morris, J. Čejka, *Chem. Soc. Rev.* (2015), <http://dx.doi.org/10.1039/C5cs0045a>.
- [19] O.V. Shvets, N. Kasián, A. Zukal, J. Pinkas, J. Čejka, *Chem. Mater.* 22 (2010) 3482–3495.
- [20] M. Taramasso, G. Perego, B. Notari, in: H. Robson (Ed.), *Verified Syntheses of Zeolitic Materials*, Elsevier, Amsterdam, 2001, p. 207.
- [21] W. Schmidt, in: V. Valtchev, S. Mintova, M. Tsapatsis (Eds.), *Ordered Porous Solids: Recent Advances and Prospects*, Elsevier, Amsterdam, 2009, pp. 51–75.
- [22] B.C. Lippens, J.H. de Boer, *J. Catal.* 4 (1965) 319.
- [23] Ch. Baerlocher, L.B. McCusker, Database of Zeolite Structures, <http://www.iza-structure.org/databases/> (downloaded on 26.6.15).
- [24] A. Thangaraj, S. Sivasanker, *J. Chem. Soc. Chem. Commun.* (1992) 123.
- [25] A. Zukal, M. Kubů, *Dalton Trans.* 43 (2014) 10558–10565.
- [26] F. Bonito, A. Damini, G. Ricchardini, M. Ricci, G. Spano, R. D'Aloisio, A. Zecchina, C. Lamberti, C. Prestipino, S. Bordiga, *J. Phys. Chem. B* 108 (2004) 3573–3583.
- [27] A. Zecchina, G. Spoto, S. Bordiga, A. Ferrero, G. Petrini, G. Leofanti, M. Padovan, in: P.A. Jacobs, N.I. Jaeger, L. Kubelková, B. Wichterlová (Eds.), *Stud. Surf. Sci. Catal.* 69 (1991) 251–258.
- [28] R. Millini, E. Previde Massara, G. Perego, G. Bellussi, *J. Catal.* 137 (1992) 497–503.
- [29] P. Ratnasamy, D. Srinivas, H. Knozinger, *Adv. Catal.* 48 (2004) 1–169.
- [30] J. Přech, D. Vítvarová, L. Lupinková, M. Kubů, J. Čejka, *Micropor. Mesopor. Mater.* 212 (2015) 28–34.
- [31] M. Sasaki, Y. Sato, Y. Tsuboi, S. Inagaki, Y. Kubota, *ACS Catal.* 4 (2014) 2653–2657.
- [32] Q. Guo, K. Sun, Z. Feng, G. Li, M. Guo, F. Fan, C. Li, *Chem. Eur. J.* 18 (2012) 13854–13860.
- [33] J.C. van der Waal, H. van Bekkum, *J. Mol. Catal. A: Chem.* 124 (1997) 137–146.
- [34] C. Pirovano, M. Guidotti, V. Dal Santo, R. Psaro, O.A. Kholdeeva, I.D. Ivanchikova, *Catal. Today* 197 (2012) 170–177.
- [35] A. Corma, M. Iglesias, F. Sánchez, *J. Chem. Soc. Chem. Commun.* (1995) 1635.